THE REUVEN RAMATY HIGH-ENERGY SOLAR SPECTROSCOPIC IMAGER (RHESSI)

R. P. LIN[1,2], B. R. DENNIS[3], G. J. HURFORD[1], D. M. SMITH[1], A. ZEHNDER[4],
P. R. HARVEY[1], D. W. CURTIS[1], D. PANKOW[1], P. TURIN[1], M. BESTER[1],
A. CSILLAGHY[1,9], M. LEWIS[1], N. MADDEN[5], H. F. VAN BEEK[6], M. APPLEBY[7],
T. RAUDORF[8], J. McTIERNAN[1], R. RAMATY[3,10], E. SCHMAHL[3,15],
R. SCHWARTZ[3,16], S. KRUCKER[1], R. ABIAD[1], T. QUINN[1], P. BERG[1], M. HASHII[1],
R. STERLING[1], R. JACKSON[1], R. PRATT[1], R. D. CAMPBELL[1,10], D. MALONE[1],
D. LANDIS[1], C. P. BARRINGTON-LEIGH[1], S. SLASSI-SENNOU[1], C. CORK[5],
D. CLARK[3], D. AMATO[3], L. ORWIG[3], R. BOYLE[3], I. S. BANKS[3], K. SHIREY[3],
A. K. TOLBERT[3,16], D. ZARRO[3,26], F. SNOW[3], K. THOMSEN[4], R. HENNECK[4],
A. MCHEDLISHVILI[4], P. MING[4], M. FIVIAN[1,11], JOHN JORDAN[12],
RICHARD WANNER[12], JERRY CRUBB[12], J. PREBLE[12,13], M. MATRANGA[12,14],
A. BENZ[17], H. HUDSON[1], R. C. CANFIELD[18], G. D. HOLMAN[3], C. CRANNELL[3],
T. KOSUGI[19], A. G. EMSLIE[20], N. VILMER[21], J. C. BROWN[22], C. JOHNS-KRULL[23],
M. ASCHWANDEN[24], T. METCALF[24] and A. CONWAY[25]

[1]*Space Sciences Laboratory, University of California Berkeley, Berkeley, CA 94720-7450, U.S.A.*
[2]*Physics Department, University of California, Berkeley CA 94720–7300, U.S.A.*
[3]*NASA/Goddard Space Flight Center, Greenbelt, MD 20771, U.S.A.*
[4]*Paul Scherrer Institut (PSI), CH-5232 Villigen PSI, Switzerland*
[5]*Lawrence Berkeley National Laboratory, Berkeley, CA 94720, U.S.A.*
[6]*H. F. van Beek Consultancy (VBC), 3971 LB Driebergen, The Netherlands*
[7]*Tecomet, Woburn, MA 01801, now at Mikro Systems Inc., Charlottesville, VA, U.S.A.*
[8]*Ortec, Oak Ridge, TN 37831–0895*
[9]*University of Applied Sciences, CH-5210 Windisch, Switzerland*
[10]*Deceased*
[11]*Previously PSI*
[12]*Spectrum Astro, Gilbert, AZ 85233, U.S.A.*
[13]*SpaceWorks Inc., Carefree, AZ 85377–2014, U.S.A.*
[14]*The Charles Stark Draper Laboratory Inc., Cambridge, MA 02139–3563, U.S.A.*
[15]*Universtity of Maryland, College Park, MD 20742, U.S.A.*
[16]*Science Systems & Applications Inc. (SSAI), Lanham, MD 20771, U.S.A.*
[17]*ETHZ, Zürich CH-8092, Switzerland*
[18]*Montana State University, Bozeman, MT 59717, U.S.A.*
[19]*ISAS, Sagamihara City, Kanagawa Prefecture, Japan*
[20]*University of Alabama in Huntsville, Huntsville, AL 35899, U.S.A.*
[21]*Observatoire de Paris-Meudon, France*
[22]*University of Glasgow, Glasgow G128QW, Scotland, U.K.*
[23]*Rice University, Houston, TX 77005, U.S.A.*
[24]*Lockheed-Martin, Palo Alto, CA 94304, U.S.A.*
[25]*The Open University, Milton Keynes MK7 6AA, U.K.*
[26]*L-3 Communications, New York, NY 10016, U.S.A.*

Abstract. RHESSI is the sixth in the NASA line of Small Explorer (SMEX) missions and the first managed in the Principal Investigator mode, where the PI is responsible for all aspects of the mission except the launch vehicle. RHESSI is designed to investigate particle acceleration and energy release in solar flares, through imaging and spectroscopy of hard X-ray/gamma-ray continua emitted by energetic electrons, and of gamma-ray lines produced by energetic ions. The single instrument consists of an imager, made up of nine bi-grid rotating modulation collimators (RMCs), in front of a spectrometer with nine cryogenically-cooled germanium detectors (GeDs), one behind each RMC. It provides the first high-resolution hard X-ray imaging spectroscopy, the first high-resolution gamma-ray line spectroscopy, and the first imaging above 100 keV including the first imaging of gamma-ray lines. The spatial resolution is as fine as ~ 2.3 arc sec with a full-Sun ($\gtrsim 1°$) field of view, and the spectral resolution is $\sim 1-10$ keV FWHM over the energy range from soft X-rays (3 keV) to gamma-rays (17 MeV). An automated shutter system allows a wide dynamic range ($> 10^7$) of flare intensities to be handled without instrument saturation. Data for every photon is stored in a solid-state memory and telemetered to the ground, thus allowing for versatile data analysis keyed to specific science objectives. The spin-stabilized (~ 15 rpm) spacecraft is Sun-pointing to within $\sim 0.2°$ and operates autonomously. RHESSI was launched on 5 February 2002, into a nearly circular, 38° inclination, 600-km altitude orbit and began observations a week later. The mission is operated from Berkeley using a dedicated 11-m antenna for telemetry reception and command uplinks. All data and analysis software are made freely and immediately available to the scientific community.

1. Introduction

The processes of particle acceleration and impulsive energy release occur in active cosmic plasmas at diverse sites throughout the universe, ranging from planetary magnetospheres to active galactic nuclei. The understanding of these processes is a major goal of space physics and astrophysics, but we are just beginning to perceive the relevant basic physics. The Sun constitutes an unparalleled laboratory for investigating these processes. Its proximity allows measurements over the entire electromagnetic spectrum to be made on physically relevant scales. At the same time, the system as a whole can be studied, and escaping energetic particles and plasma can be sampled directly. Further, the complexity of solar magnetic fields and the solar atmosphere leads to a broad range of acceleration phenomena, mirroring the rich diversity of processes occurring on cosmic scales.

The primary scientific objective of RHESSI is to understand particle acceleration and explosive energy release in the magnetized plasmas at the Sun. The Sun is the most powerful particle accelerator in the solar system, accelerating ions up to tens of GeV and electrons to hundreds of MeV in solar flares and in fast coronal mass ejections (CMEs). Solar flares are the most powerful explosions, releasing up to $10^{32}-10^{33}$ ergs in 10^2-10^3 s. The flare-accelerated $\sim 10-100$ keV electrons (and sometimes $\gtrsim 1$ MeV nucleon ions) appear to contain a significant fraction, $\sim 10-50\%$, of this energy, indicating that the particle acceleration and energy release processes are intimately linked. How the Sun releases this energy, presumably stored in the magnetic fields of the corona, and how it rapidly accelerates electrons and ions with such high efficiency, and to such high energies, is presently unknown.
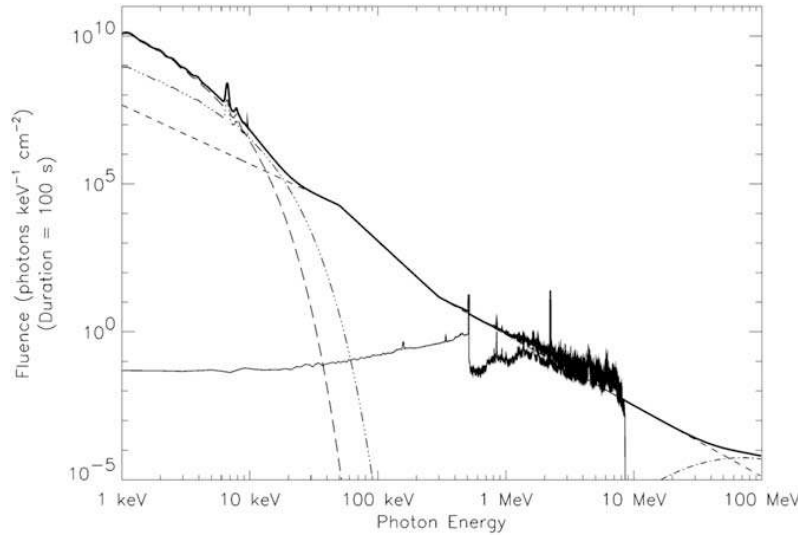
Figure 1. Composite X-ray/gamma-ray spectrum from 1 keV to 100 MeV for a large flare. At energies up to $\sim 10-30$ keV, emission from hot($\sim 10^7$ K) and 'superhot' ($\sim 3 \times 10^7$ K) thermal flare plasmas (the *two curves at the left*) dominate. Bremsstrahlung emission from energetic electrons produces the X-ray/gamma-ray continuum (*straight lines*) up to tens of MeV. Broad and narrow gamma-ray lines from nuclear interactions of energetic ions sometimes dominate the spectrum between ~ 1 to 7 MeV. Above a few tens of MeV the photons produced by the decay of pions (*curve at the right*) dominates. RHESSI observations cover almost four orders of magnitude in energy (3 keV to 17 MeV).

High-energy emissions are the most direct signature of the acceleration of electrons, protons and heavier ions in solar flares (Figure 1). Accelerated electrons colliding with the ambient solar atmosphere produce bremsstrahlung hard X-ray and gamma-ray continuum emission, while nuclear collisions of energetic ions result in a complex spectrum of narrow and broad gamma-ray lines. Hot (million-degrees) thermal flare plasmas also emit bremsstrahlung X-rays. RHESSI is designed to provide high resolution imaging and spectroscopy of all these emissions, from soft X-rays (3 keV) to gamma-rays (17 MeV).

These emissions are accompanied by longer wavelength emissions, and sometimes by escaping energetic particles. Their observation by the fleet of spacecraft (Solar and Heliospheric Observatory (SOHO), WIND, Advance Composition Explorer (ACE), *Ulysses*, Transition Region And Coronal Explorer (TRACE), Geostationary Operational Environmental Satellite Project (GOES), Solar Anomalous and Magnetospheric Particle Explorer (SAMPEX), etc.) already in place, and by ground-based instruments, provides the crucial information on the context in which the high energy processes occur.

RHESSI is the first Small Explorer mission carried out in the 'Principal Investigator-mode', where the PI and team are responsible for all aspects of the

mission except providing the launch vehicle. This includes developing, integrating, and testing the instrument and spacecraft; providing launch support, telemetry downlink and command uplink, mission and science operations, data processing and distribution; analyzing and archiving the data, and disseminating the results.

The RHESSI mission was selected by NASA in October 1997, with a very aggressive development schedule aimed at a launch in July 2000, near the predicted peak of the ~ 11-year solar activity cycle. During environmental testing of the integrated spacecraft at the Jet Propulsion Laboratory in March 2000, however, a malfunction in the shake table subjected RHESSI to a vibration level of > 25 G rather than the requested 2 G, resulting in extensive damage to both the instrument and spacecraft. At about this time the failure of a Mars orbiting mission and then a Mars lander led NASA to institute a policy of additional external 'Red Team' reviews. Even with all the extra effort involved in these reviews and the implementation of their recommendations, the instrument and spacecraft were repaired, re-integrated, and re-tested in time for a launch at the end of 2000.

A problem was then discovered on the three-stage solid-propellant Pegasus-XL launch vehicle, and fixing that problem delayed the launch to March 2001, and again to June 2001. In April 2001, the RHESSI spacecraft was integrated with the Pegasus-XL at Orbital Science Corporation's facilities in the Western Test Range, and in early June it was carried underneath an L-1011 aircraft to the Eastern Test Range at Kennedy Space Center. One week before the planned RHESSI launch, NASA attempted a test flight of the prototype X-43 aerospace plane. The modified Pegasus first stage used for launch failed and the X-43 had to be destroyed. This led to a series of further delays while the cause of the failure was investigated. Finally, on 5 February 2002, the RHESSI satellite was launched by the Pegasus-XL, following its release from the L-1011 at $\sim 40\,000$ feet altitude over the Atlantic Ocean. A near perfect, 38° inclination, 600 km altitude circular orbit was achieved.

The mission was renamed from HESSI to RHESSI after launch to honor Dr Reuven Ramaty, a distinguished theoretical high-energy astrophysicist and solar physicist working at Goddard Space Flight Center (GSFC). Dr Ramaty developed much of the theoretical framework for solar gamma-ray line spectroscopy, and he was a Co-I and a strong advocate of RHESSI. He passed away in March 2001, eight months after the planned launch date, but 11 months prior to the actual launch. He is the first NASA scientist to have a space mission named after him.

2. Scientific Objectives and Design Considerations

2.1. ACCELERATION OF ELECTRONS

Bursts of bremsstrahlung hard X-rays ($\gtrsim 20$ keV), emitted by accelerated electrons colliding with the ambient solar atmosphere, are the most common signature of the impulsive phase of a solar flare (Figure 2). Provided the electron energy E_e is much
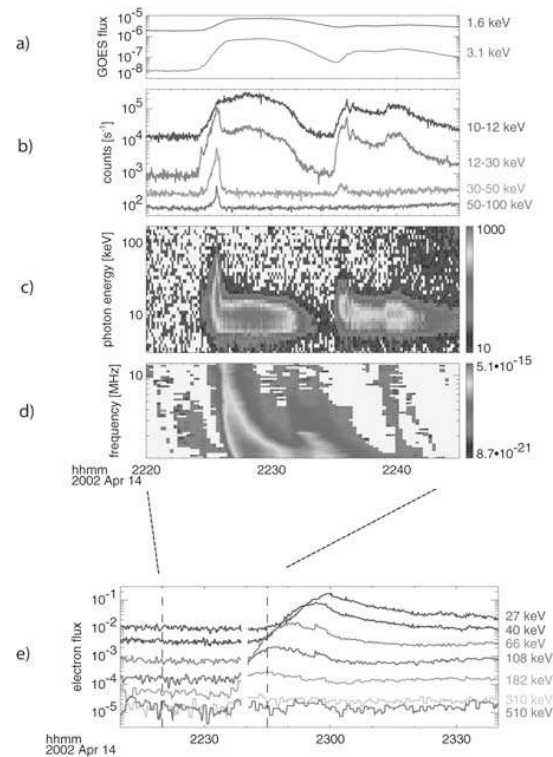
Figure 2. [See CD-ROM for color version]. Time profile of X-ray fluxes from GOES (a) and RHESSI (b); counts are multiplied by factors of 8, 50, and 500, for the 30–50 keV, 12–30 keV, and 10–12 keV channels, respectively). The next two panels show spectrograms of (c) the RHESSI counts in 20 logarithmic energy channels, and of (d) 1–14 MHz radio emission detected by the WIND spacecraft (Bougeret *et al.*, 1995). The solar flare with hard X-ray peak at ∼ 22:26 UT is accompanied by a type III solar radio burst, produced by energetic electrons escaping the Sun. The (e) bottom panel (longer time interval) shows the energetic electrons arriving at WIND at 1 AU (Lin *et al.*, 1995), with the faster electrons arriving first, consistent with an impulsive injection of the electrons from the Sun at the time of the X-ray peak.

greater than the average thermal energy, kT, of the ambient gas, essentially all of the electron energy will be lost to Coulomb collisions, with only a tiny fraction ($\sim 10^{-5}$) lost to bremsstrahlung. For this non-thermal situation, the hard X-ray fluxes observed in many flares indicate that the energy in accelerated > 20 keV electrons must be comparable to the total flare radiative and mechanical output (Lin and Hudson, 1976). Thus, the acceleration of electrons to tens of keV may be the most direct consequence of the basic flare-energy release process.

High-resolution hard X-ray imaging spectroscopy is the key to understanding the electron acceleration and energy release processes in solar flares. High-spectral-

resolution measurements of the solar flare hard X-ray spectrum can be directly inverted to obtain the detailed spectrum of the parent X-ray-producing electrons (Johns and Lin, 1992). RHESSI is designed to provide imaging spectroscopy – the photon spectrum is obtained in each spatial element (Figure 3) as a function of time. In principle, this spectrum provides detailed information on $N(E, \mathbf{r}, t)$, the X-ray producing electron number density, as a function of energy (E), position ($\mathbf{r}$), and time (t). With information from context observations on the ambient density, temperature, magnetic field strength and topology, the electron loss processes can be directly evaluated to determine whether the X-ray emission is thermal or non thermal. By using a spatially dependent continuity equation, including loss processes, the spatially and temporally resolved accelerated electron source distribution, $F(E, \mathbf{r}, t)$, can be inferred. Then, detailed quantitative models of the acceleration, energy release, and energy propagation processes can be constructed and tested.

RHESSI is designed to provide spatial (Figure 4(b)) and temporal resolution commensurate with the spatial and temporal scales for the accelerated electrons to lose their energy in the lower corona and upper chromosphere (ambient densities below $\sim 10^{12}$ cm^{-3}). To resolve the very steep thermal spectra and determine the lower energy limit of the non-thermal spectrum (critical to determining the energy content in fast electrons), ~ 1 keV spectral resolution (Figure 4(a)) is needed. The energy range should extend low enough so the thermal–nonthermal transition can be determined, and as high as practical, but certainly up to relativistic energies where a different acceleration process may be operating. Finally, high sensitivity is required to detect microflares (which may be important for coronal heating), and very wide dynamic range is required to make measurements in the largest flares without saturation.

2.2. ACCELERATION OF IONS

Near the Sun, nuclear collisions of accelerated ions with the ambient solar atmosphere result in a rich spectrum (Figure 1) of gamma-ray lines (Ramaty and Murphy, 1987; Chupp, 1990, Share and Murphy, 1995). Energetic protons and alpha-particles colliding with carbon and heavier nuclei produce narrow de-excitation lines (widths of $\sim$ few keV to ~ 100 keV), while energetic heavy nuclei colliding with ambient hydrogen and helium produce much broader lines (widths of hundreds of keV to an MeV). Neutron capture on hydrogen and positron annihilation produce delayed narrow lines, at 2.223 MeV and 0.511 MeV, respectively.

The bulk of the gamma-ray line emission is produced by ions with energies of 10–100 MeV nucleon that contain only a small fraction of the energy in the $\gtrsim 20$ keV electrons. However, systematic study of SMM gamma-ray line flares (Share and Murphy, 1995) showed that the 1.634 MeV ^{20}Ne line is enhanced relative to other lines. Because the cross section for ^{20}Ne has an unusually low energy threshold (~ 2.5 MeV), this effect appears to be due to large fluxes of low-energy
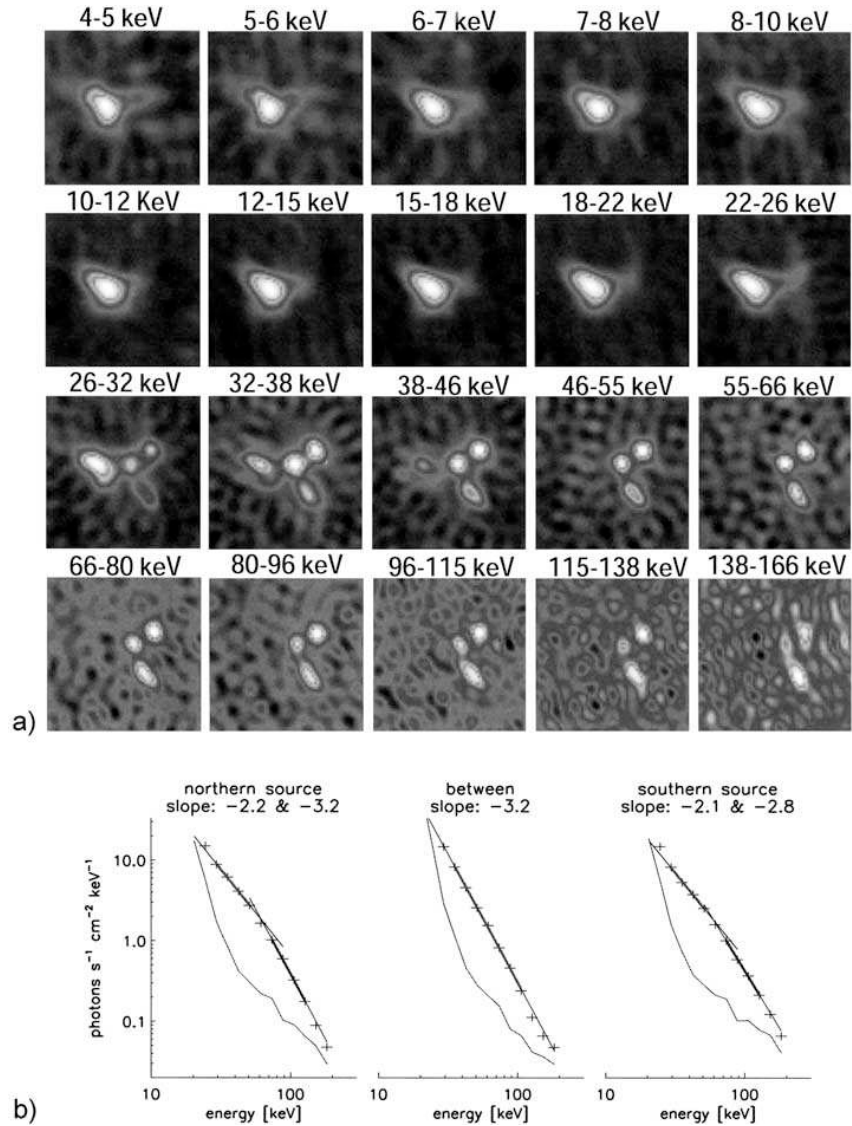
Figure 3. [See CD-ROM for color version]. (a) Imaging of the July 23, 2002, X4.8 solar flare in 20 energy bands, from 1 keV wide bins at 4 keV, to 28 keV wide bins (for enough counts to image) at 138 keV, illustrating the changes in sources as a function of energy, from a single dominant elongated source at energies below ~ 30 keV to three sources above ~ 40 keV. The images are 64 arc sec on a side; the lower left corner is just at the southeast limb of the Sun. (b) The energy spectra of the three dominant sources at energies above ~ 40 keV, showing that the spectra are similar for the north and south sources but quite different for the source in between. The *dashed lines* indicate background.
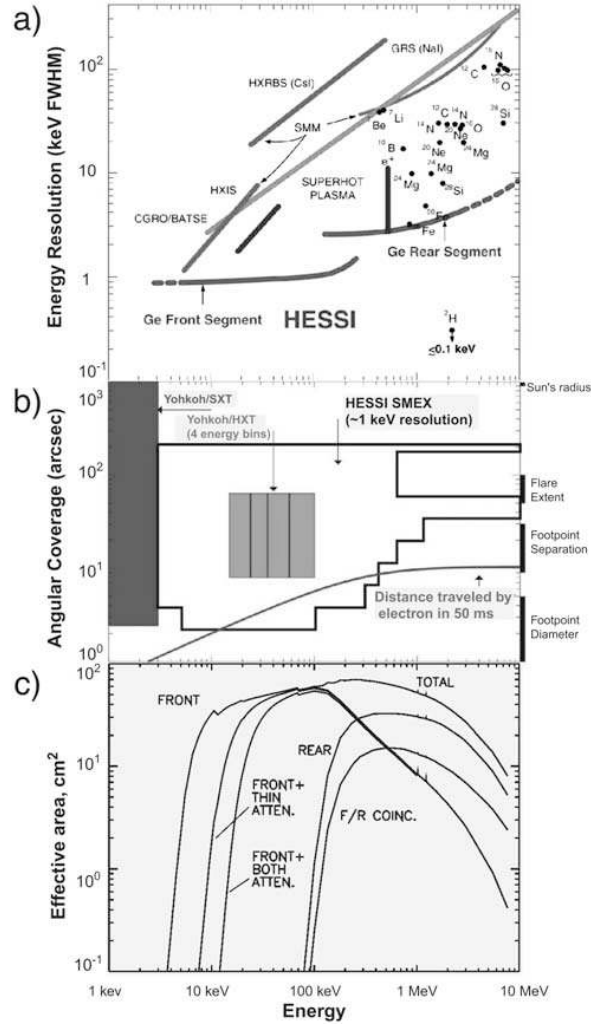
Figure 4. [See CD-ROM for color version]. (a) RHESSI's Full Width at Half Maximum (FWHM) energy resolution (*lower curves*), compared with previous instruments (*upper lines*). The *dots* are the expected FWHM widths of the predicted gamma-ray lines, and the *vertical line* the range of widths (temperature and density dependent) for the positron annihilation line. The *short diagonal line* shows the resolution needed to resolve the steep 'superhot thermal' emission. (b) RHESSI's angular resolution versus energy, compared to *Yohkoh* Soft X-ray Telescope (SXT) (*left*) and Hard X-ray Telescope (HXT) (*center*). RHESSI has ~ 1–10 keV energy resolution over this energy range and can image up to 17 MeV, while HXT had four broad energy channels from 15 to 100 keV. (c) RHESSI's effective (photopeak) area as a function of energy for solar X-rays/gamma-rays. The *three curves to the left* show the effect on the front segment response (summed over all nine detectors) of no attenuators, thin attenuator, or both thick and thin attenuator inserted over the detectors. The *curves to the right* show the effective area for the rear segment, and for photons that leave energy in both the front and rear segment of the detectors (F/R coincidence).

ions with total energy content often comparable to that of the accelerated electrons (Ramaty *et al.*, 1995; Emslie *et al.*, 1997).

RHESSI is designed to probe ion acceleration with the first high-resolution spectroscopy of solar flare gamma-ray lines (Figure 4(a)), giving the first detailed line shapes, which depend on the angular distribution of the interacting accelerated ions. The shape of the 0.511 MeV positron annihilation line gives information about the density and temperature of the ambient medium since the positrons slow down before annihilating. The high resolution enables closely spaced lines to be separated, particularly important around 1 MeV, where several lines are produced by accelerated ^{3}He. Their detection would test whether gamma-ray flares and impulsive, ^{3}He-rich solar energetic particle events have a common origin (Ramaty *et al.*, 1993).

RHESSI is also designed to image solar flare gamma-ray lines (Figure 4(b)), thus providing the first information on the locations of energetic heavy ions and protons and their secondary neutrons and positrons, to compare with the location of the energetic electrons. The instrument's high spectral resolution allows imaging in narrow gamma-ray lines, such as the 2.223 MeV neutron capture line, where line counts dominate over the background. The continuum above ~ 1 MeV (especially $4-7$ MeV) is often dominated by the broad lines from accelerated heavy ($Z > 2$) ions, and can be imaged to locate them. In a very large gamma-ray line flare with good statistics, the > 2.5 MeV protons might be located by imaging the ^{20}Ne de-excitation line.

2.3. Non-solar science

Although designed as a solar instrument, RHESSI's lack of shielding around the detectors (to minimize weight) makes it an effective high-spectral-resolution ($\sim$ keV FWHM), wide-field-of-view hard X-ray/gamma-ray all-sky monitor, with ~ 150 cm^2 collecting area. The spacecraft's rotation produces many detector/detector occultations per minute, and two brief Earth occultation/deoccultations occur per orbit (Harmon *et al.*, 1992; Zhang *et al.*, 1993), allowing localization of transients (black-hole X-ray novae, Be/neutron star binary outbursts, etc.) and steady sources. RHESSI is able to resolve cyclotron absorption features from bright transients such as A0535+26, search for line features in gamma-ray bursts, and study the Galactic positron annihilation and ^{26}Al decay lines from nucleosynthesis in supernovae and massive stellar systems on large angular scales. RHESSI can image the Crab Nebula once a year (when it approaches within 1.6° of the Sun), with unprecedented spatial (2.3 arc sec) and energy (~ 1 keV) resolution in hard X-rays. RHESSI also provides high spectral and temporal resolution measurements of terrestrial X-ray/gamma-ray continuum emissions from electron precipitation, of terrestrial gamma-ray line emission from the impact of cosmic rays and solar energetic particles, and of gamma-ray bursts associated with lightning (Fishman *et al.*, 1994).

3. Instrument

The RHESSI scientific objectives are achieved with high-resolution imaging spectroscopy observations from soft X-rays to gamma-rays, utilizing a single instrument consisting of an Imaging System, a Spectrometer, and the Instrument Data Processing Unit (IDPU) containing the instrument electronics. An instrument schematic is shown in Figure 5 and the specifications are given in Table Ia. The Imaging System is made up of nine Rotating Modulation Collimators (RMCs), each consisting of a pair of widely separated grids mounted on a rotating spacecraft. Pointing information is provided by the Solar Aspect System (SAS) and redundant Roll Angle Systems (RASs). The Spectrometer has nine segmented germanium detectors (GeDs), one behind each RMC, to detect photons from 3 keV to 17 MeV. The GeDs are cooled to $\lesssim 75$ K by a space-qualified long-life mechanical cryocooler, to achieve the highest spectral resolution (Figure 4(b)) of any presently available gamma-ray detector. As the spacecraft rotates, the RMCs convert the spatial information from the source into temporal modulation of the photon counting rates of the GeDs. The instrument electronics amplify, shape, and digitize the GeD signals, provide low-voltage power and GeD high voltage, format the data, and interface to the spacecraft electronics.

The energy and arrival time of every photon, together with aspect data, are recorded in the spacecraft's on-board 4-Gbyte solid-state memory (sized to hold all the data from the largest flare) and automatically telemetered within 48 hours. With these data, the X-ray/gamma-ray images can be reconstructed on the ground (see Figure 3). The instrument's $\sim 1°$ field of view is much wider than the $\sim 0.5°$ solar diameter, so all flares are detected, and pointing can be automated.

3.1. IMAGING SYSTEM

A detailed description of the RHESSI imaging technique is given in Hurford *et al.* (2002). At hard X-ray and gamma-ray energies, unlike soft X-rays, EUV, and longer wavelength emissions, focusing optics are not feasible. The only viable method of obtaining arcsecond-class images in hard X-rays and gamma-rays within the Small Explorer constraints is with Fourier-transform imaging, similar to that used in the pioneering *Hinotori* rotating modulation collimator (Makishima *et al.*, 1977) and *Yohkoh* Hard X-ray Telescope (HXT) (Kosugi *et al.*, 1991). RHESSI uses nine collimators, each made up of a pair of widely separated grids. Each grid is a planar array of equally-spaced, X-ray-opaque slats separated by transparent slits (Figure 6). The slits of each pair of grids are parallel to each other and their pitches (p) are identical, so that the transmission through the grid pair depends on the direction of the incident X-rays. For slits and slats of equal width, the transmission is modulated from zero to 50% and back to zero for a change in source angle to collimator axis (orthogonal to the slits) of p/L where L is the separation between grids. The angular resolution is then defined as $p/(2L)$.

TABLE I
RHESSI characteristics.

Ia. Instrument characteristics:

Energy range	3 keV to 17 MeV
Energy resolution (FWHM)	$\lesssim 1$ keV at 3 keV, increasing to ~ 5 keV at 5 MeV
Angular resolution	2.3 arc sec to 100 keV, 7 arc sec to 400 keV, 36 arc sec to 15 MeV
Temporal resolution	2 s for detailed image, tens of ms for basic image
Field of view	full Sun ($\sim 1°$)
Effective area (photopeak)	$\sim 10^{-3}$ cm^2 at 3 keV, ~ 32 cm^2 at 10 keV (with attenuators out), ~ 60 cm^2 at 100 keV, ~ 15 cm^2 at 5 MeV
Detectors	9 germanium detectors (7.1-cm dia. $\times$ 8.5 cm), cooled to < 75 K with Stirling-cycle mechanical cooler
Imager	9 pairs of grids, with pitches from 34 microns to 2.75 mm, and 1.55-m grid separation
Aspect system	Solar Aspect System: Sun center to < 1 arc sec Roll Angle System: roll to ~ 1 arc min
Number of flares expected	~ 1000 imaged to > 100 keV $\sim$ tens with spectroscopy to ~ 10 MeV

Ib. Spacecraft characteristics:

Mass	Total 291.1 kg, instrument 130.8 kg
Power	Total 220.4 W, instrument 142.3 W
Size	1.18 m diameter, 2.06 m height, 5.74 m tip-to-tip with solar panels deployed
Telemetry	4 Mbps, downlink, 2 kbps command uplink
On-board storage	4 Gbyte solid state memory
Attitude	15 rpm spin rate, pointing to 0.2° of Sun center

Ic. Mission characteristics:

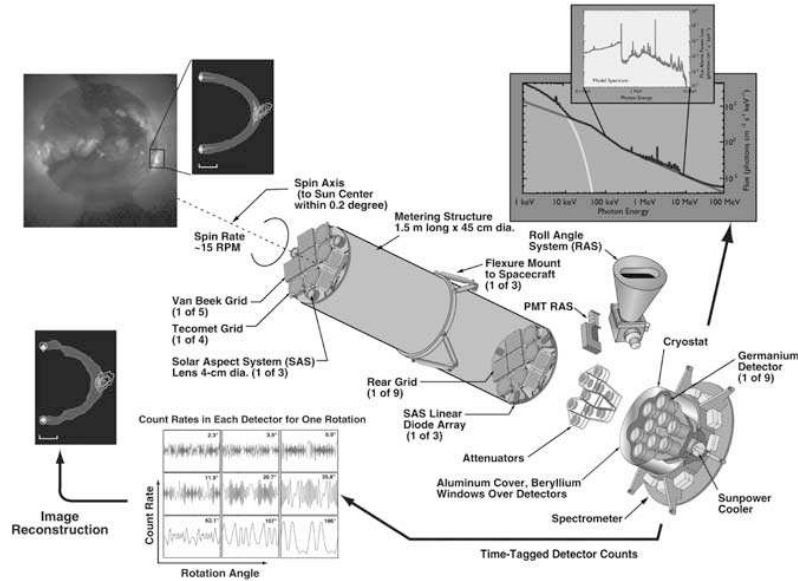|	
Launch date	5 February 2002
Launch vehicle	Pegasus XL
Orbit	38° inclination, 600 km altitude apogee, 586 km perigee
Nominal mission lifetime	2 years, 3rd year highly desirable

Figure 5. [See CD-ROM for color version]. Schematic of the RHESSI instrument illustrating the imaging spectroscopy. X-rays and gamma-rays from the Sun (*upper left*) pass through the slits of the front and rear grids of each of the nine grid pairs to reach the germanium detector. As the spacecraft rotates the detector count rates are temporally modulated (*lower left*). These modulations can be analyzed to reconstruct the image. The germanium detectors are cryogenically cooled to provide high spectral resolution capable of resolving narrow gamma-ray lines and steep solar continuum spectra (*upper right*). The attenuators are inserted automatically when the count rate approaches saturation. The SAS, RAS and PMTRAS provide solar pointing and roll aspect information.

For RHESSI, the transmission of the source photons through the grids is modulated by mounting the instrument on a rotating spacecraft. The X-ray/gamma-ray detector behind the collimator records the arrival time and energy of individual photons, allowing the modulated counting rate to be determined as a function of rotation angle. Note that the detector does not need to have any spatial resolution and hence can be optimized for high sensitivity and energy resolution.

For a parallel incident beam, the modulated waveform generated by a smoothly rotating spacecraft has a distinctive quasi-triangular shape locally. The amplitude is proportional to the intensity of the beam, and the phase and frequency depend on the direction of incidence. For complex sources, and over small rotation angles, the amplitude and phase of the waveform provide a direct measurement of a single Fourier component of the angular distribution of the source (e.g., Prince *et al.*, 1988). Different Fourier components are measured at different rotation angles and with grids of different pitches. For RHESSI, the separation between grids in each RMC is L = 1.55 m and the grid pitches range from $p = 34$ μm to 2.75 mm in steps
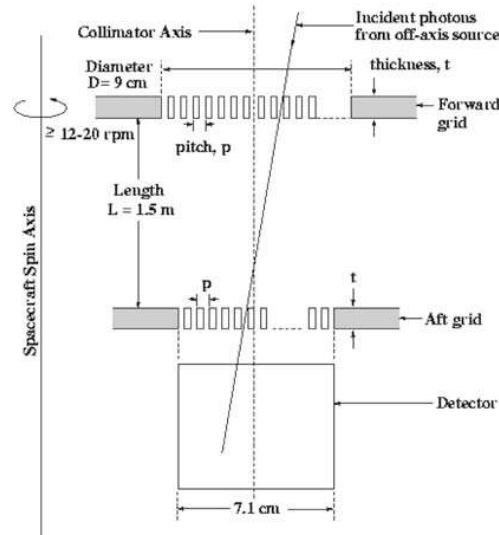
Figure 6. Schematic showing the parameters that define the imaging capability.

of $\sqrt{3}$. This provides angular resolutions spaced logarithmically from 2.3 arc sec to $\gtrsim 3$ arc min, allowing sources to be imaged over a wide range of angular scales. Diffuse sources larger than 3 arc min are not imaged but full spectroscopic information is still obtained. Multiple smaller sources are imaged regardless of their separation.

In a half rotation (2 s), the nine RMCs measure amplitudes and phases of ~ 1100 Fourier components for a typical source location, compared to 32 Fourier components for the *Yohkoh* HXT, so that far more complex flare images can be resolved. Although one half rotation is required to measure a full set of Fourier components, the measurement of each component takes only a single modulation cycle, which can be as short as 1.3 ms for the finest grids. Thus, when count rates are sufficiently high, crude images (from about ten Fourier components) can be obtained, in principle, on timescales of tens of milliseconds.

Changing the separation (L) between grids or displacing the grids parallel to the slits has little effect on imaging performance. A relative displacement perpendicular to the slits affects the phase but not the amplitude of modulation. Any such displacement will be accurately monitored by the SAS, and can be fully compensated for in the image reconstruction process. The critical alignment requirement is associated with the rotation or twist of one grid with respect to the other about the line of sight to the source. A relative twist of p/D (D = diameter of grid) reduces the modulated amplitude almost to zero. Thus, the grid pairs must be well aligned in twist throughout the mission. For the finest grids (2.3 arc sec resolution) a 1-arc min alignment is needed. Thus, HESSI can achieve arc-sec-quality images with

an instrument having only arc-min alignment requirements. To minimize twist, the grids are aligned and mounted precisely on grid trays which are attached to opposite ends of a graphite-epoxy support tube.

3.1.1. *Grids*

The main challenges in fabricating the RHESSI grids were: (i) the extremely fine slit and slat widths (20 and 14 microns for 34 micron pitch) required for the finest grid, (ii) the high (50 : 1) aspect ratio of the slit width to grid thickness for maximum absorption consistent with a $\sim$ 1° field of view, and (iii) the fine tolerance on the relative pitches of the two grids in each pair ($<$ 1 part in 20 000 for the finest grid pair). Tecomet, Inc., fabricated the four finest grid pairs (plus a third spare grid) using a foil stacking method in which thin sheets of metal were photo-etched and precision stacked with epoxy bonding to produce a solid structure (Figure 7(a), left). Tungsten was used for all of the grids except for the finest; grid pair 1 (Figure 7(b)) was made of molybdenum (sufficiently thin tungsten sheets were not available then), resulting in a maximum energy for modulation of $\sim$ 100 keV, rather than $\sim$ 200 keV had it been tungsten. The five coarsest grid pairs were made by van Beek Consultancy in The Netherlands using tungsten blades packed together side by side with spacers in between (Figure 7(a), right) to give the required, pitch, slit width, and grid thickness. The thickest grids, No. 6 (Figure 7(c)) and 9 (1.85 and 3 cm thick) were designed to modulate gamma-rays up to 17 MeV (Figure 4(b)).

All the grids were fully characterized at GSFC both optically and using X-rays. Optical images were taken at high magnification of the front and rear of each grid using a customized facility. Each grid was mounted on an XY table with laser readout, and measurements of the pitch, phase, and orientation of the slits in each grid were obtained with micron positional accuracy. A separate X-ray characterization facility determined the average X-ray transmission of each flight grid as a function of photon energy and angle from grid normal. In addition, the variation of this transmission across the full area of each grid was measured with $\sim$ 1-cm resolution.

All grids were also fully flight qualified at GSFC by vibration testing and thermal cycling to GEVS (General Environmental Verification Specification) standards. The grids were then transported to Paul Scherrer Institut (PSI) in Switzerland where they were mounted and aligned on the front and rear end trays. Precision coordinate measurement machines were used to establish and verify the correct alignment of each grid pair, so that in the final assembly the slits of the front and rear grids of each pair would be parallel to within the very strict tolerances required for modulation of the incident photon flux.

After assembly of the trays onto the imager tube at PSI, an end-to-end check on the grid alignments was carried out. Since an X-ray beam parallel to $\lesssim$ 1 arc sec could not be obtained, a radioactive ^{109}Cd source was placed behind the spare grid for each pair, to provide a series of diverging fan beams of 22 keV X-rays. By moving this source/grid while maintaining an appropriate distance from the grid
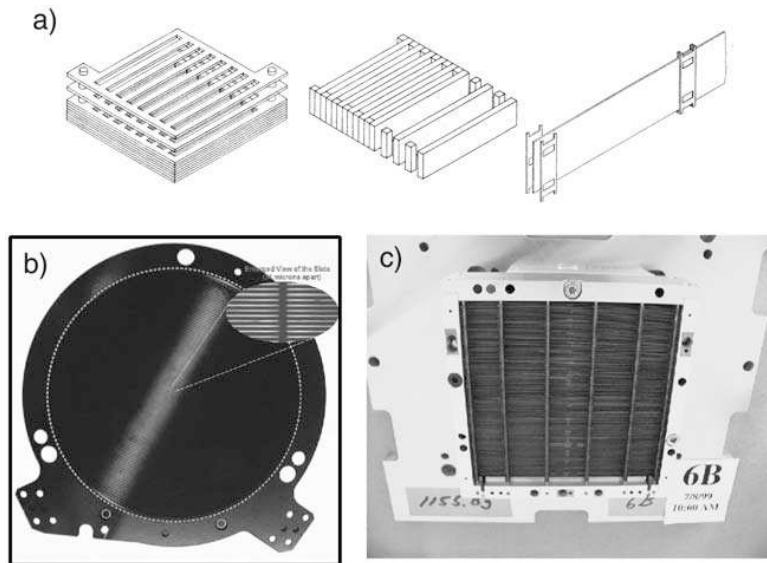
Figure 7. [See CD-ROM for color version]. (a) Schematic of the two grid fabrication processes: left, stacking etched foils and epoxying them to obtain the required thickness; middle and right, packing vertical blades with spacers in between. (b) Photograph of a grid No. 1 showing the slits and bridges in the insert. (c) Photograph of flight grid No. 6.

pair, a modulation in transmission would be detected providing that the two grids of that pair were correctly aligned. This test was carried out on all but the two coarsest grid pairs – their alignments could be checked visually.

For long-term monitoring of the grid alignment through all testing and environmental qualification prior to launch, an optical twist monitoring system (TMS) was used repeatedly. This system relied on optical photodiodes mounted behind pinholes in the rims of the rear grids. The light from these photodiodes passed through annuli mounted in the front grids in such a way that the diffracted beams from any one grid pair converged onto a Charge Couple Device (CCD) camera mounted at the appropriate distance in front of the telescope assembly. The positions of the converging beams as determined from the images provided an accurate measure of any change in the relative twist of the front and rear grids of a each pair. In this way, the correct alignment of even the finest grid pair could be verified up to launch. No significant change in alignment was ever measured except after the vibration accident at Jet Propulsion Laboratory (JPL), when the front grid No. 6 was hit and moved on its mount. The complete imaging telescope system was shipped back to PSI, a new mount installed for the front grid 6, and all grid alignments were rechecked and verified, including repeating the TMS check.